Damage Quantification in Electrically Conductive Composite Laminate Structures

Alexander S. Liberson, Brian R.Walsh and Michael J. Roemer
Impact Technologies LLC
200 Canal View Blvd
Rochester, NY 14618

Gyaneshwar P. Tandon and Ran Y. Kim
University of Dayton Research Institute
300 College Park
Dayton, OH 45469-0168

Abstract

This paper presents an approach for assessing damage in electrically conductive reinforced polymers that is based on feature changes in the current flow and overall conductivity of the structure under damage conditions such as internal fiber fracture and delamination cracks. Through monitoring the integral resistance of the structure, changes in a selected feature set related to the inherent conductivity is directly correlated to the location and extent of the damage present.

The technique employed uses a relatively simple analysis process and requires a network of electrodes to apply electric potential to the external surfaces of the structure. A Finite Element Model (FEM) of the structure enables the calculation of the predicted electrostatic environment inside multidirectional laminates with highly anisotropic plies. Orientation of the electrically conductive fibers is accounted for by introducing the corresponding anisotropic conductivity tensor for each ply. Multiple parametric analyses of unidirectional and multidirectional laminates show significant influence of anisotropy on current flow trajectories, and overall resistivity.

The influence of holes, cracks and delaminations have been determined by measurements and compared with the theoretical FEM model results. A comparison of the potential and current distribution for damaged and undamaged laminates shows a substantial difference around the damaged area, as well as the difference in a set of overall resistivities. The difference induced by small cracks produces subtle deviations in measurements. The corresponding sensitivities are used to deduce the requirement precision of the measurement instrument, which forms the basis of a damage detection system.

Finally, selected experimental results are provided that verify the basis of the model-based analysis technique presented. Subsequently, the results are used as inputs to a lookup table based inversion scheme and training data for an artificial neural network, which are used to predict damage severity in the electrically conductive laminates.

Report Documentation Page		*Form Approved* *OMB No. 0704-0188*

1. REPORT DATE **2009**	2. REPORT TYPE	3. DATES COVERED **00-00-2009 to 00-00-2009**

4. TITLE AND SUBTITLE **Damage Quantification in Electrically Conductive Composite Laminate Structures**	5a. CONTRACT NUMBER
	5b. GRANT NUMBER
	5c. PROGRAM ELEMENT NUMBER
6. AUTHOR(S)	5d. PROJECT NUMBER
	5e. TASK NUMBER
	5f. WORK UNIT NUMBER
7. PERFORMING ORGANIZATION NAME(S) AND ADDRESS(ES) **Impact Technologies LLC,200 Canal View Blvd,Rochester,NY,14618**	8. PERFORMING ORGANIZATION REPORT NUMBER
9. SPONSORING/MONITORING AGENCY NAME(S) AND ADDRESS(ES)	10. SPONSOR/MONITOR'S ACRONYM(S)
	11. SPONSOR/MONITOR'S REPORT NUMBER(S)

12. DISTRIBUTION/AVAILABILITY STATEMENT **Approved for public release; distribution unlimited**

13. SUPPLEMENTARY NOTES

14. ABSTRACT **see report**

15. SUBJECT TERMS

16. SECURITY CLASSIFICATION OF:			17. LIMITATION OF ABSTRACT	18. NUMBER OF PAGES	19a. NAME OF RESPONSIBLE PERSON
a. REPORT **unclassified**	b. ABSTRACT **unclassified**	c. THIS PAGE **unclassified**	**Same as Report (SAR)**	**9**	

1.0 Formulation of the effective three-dimensional problem for electrically conductive anisotropic laminate composites

Consider the electrical conduction in a three-dimensional media, governed by the constitutive equations

$$\vec{J}(x) = \hat{\sigma}(x) \cdot \vec{E}(x), \qquad \nabla \cdot \vec{J} = I, \qquad \nabla \times \vec{E} = 0 \qquad (1)$$

where $\vec{J}(x)$ is the current field, $\hat{\sigma}(x)$ is the anisotropic electric conductivity tensor, $\vec{E}(x)$ is the electric field and I is the distribution of electric source current. All variables are spatially distributed as functions of position x. The first equation constitutes the Ohm's law, the second is conservation of the total current while the third corresponds to the absence of the magnetic field. Introducing electric potential (voltage) ϕ, $\vec{E}(x) = \nabla \phi$, the governing differential equations can be represented in the form

$$\nabla \cdot (\hat{\sigma} \nabla \phi) = I \qquad (2)$$

with the boundary conditions at each boundary point: Neiman: $\nabla \phi \cdot \vec{n} = 0$, or Dirichlet: $\phi = \phi^*$, or periodicity in a case of a body of revolution, $\phi(x) = \phi(x + l)$. In the case of anisotropic conductivity current density, J is not in general collinear to the vector of electric field E. Let $\hat{\sigma}'$ and $\hat{\sigma}$ denote conductivities, defined by its components, specified in a local "orthotropic" system of coordinates (x_1, x_2, x_3) for the current ply, and global coordinates (x, y, z)

$$\hat{\sigma}' = \begin{bmatrix} \sigma_{11} & \sigma_{12} & 0 \\ \sigma_{12} & \sigma_{22} & 0 \\ 0 & 0 & \sigma_{33} \end{bmatrix} \qquad \hat{\sigma} = \begin{bmatrix} \sigma_{xx} & \sigma_{xy} & 0 \\ \sigma_{xy} & \sigma_{yy} & 0 \\ 0 & 0 & \sigma_{zz} \end{bmatrix} \qquad (3)$$

Components of the second rank tensor can be transformed according to the following ($m = \cos(\theta)$, $n = \sin(\theta)$, where θ is the angle between the global x and local x_1 axes)

$$\sigma_{xx} = \sigma_{11} m^2 + \sigma_{22} n^2 - 2\sigma_{12} mn; \qquad \sigma_{yy} = \sigma_{22} m^2 + \sigma_{11} n^2 + 2\sigma_{12} mn;$$

$$\sigma_{xy} = (\sigma_{11} - \sigma_{22}) mn + 2\sigma_{12}(m^2 - n^2); \qquad \sigma_{zz} = \sigma_{33} \qquad (4)$$

Usually elementary plies are arranged in a sequence of $\pm \theta$ orientations creating a symmetrically laminated structure. Neglecting the difference of a voltage gradient between two sequential plies, the effective conductivity tensor for a symmetric laminate therefore reduce to

$$\sigma_{xx} = \sigma_{11} m^2 + \sigma_{22} n^2; \qquad \sigma_{yy} = \sigma_{22} m^2 + \sigma_{11} n^2;$$

$$\sigma_{xy} = 2\sigma_{12}(m^2 - n^2); \qquad \sigma_{zz} = \sigma_{33} \qquad (5)$$

To apply finite element simulations, equations (2) can be re-written in the following form, united for the cylindrical and Cartesian system of coordinates,

$$\frac{\partial}{\partial x}[(\sigma_{xx}\frac{\partial\varphi}{\partial x}+\sigma_{x\vartheta}\frac{\partial\varphi}{r^k\partial\vartheta})]+\frac{\partial}{r^k\partial\vartheta}[(\sigma_{\vartheta\vartheta}\frac{\partial\varphi}{r^k\partial\vartheta}+\sigma_{x\vartheta}\frac{\partial\varphi}{r^k\partial x})]+\frac{1}{r^k}\frac{\partial}{\partial r}(r^k\frac{\partial(\sigma_{rr}\varphi)}{\partial r})=I \quad (6)$$

where k=1 for cylindrical , and k=0 for Cartesian coordinates (y= ϑ , z=r).

Based on equation (6), 2-D and 3-D finite element models have been developed, using bi-linear and tri-linear shape functions inside four nodes square or eight nodes cubic type elements. As an example, we consider a section of an arbitrary symmetric angle ply laminate with ply orientations [0_2,30/-30/60/-60/0_2,90_2]$_s$ with an embedded delamination at the 60/-30 ply interface, as shown in Figure 1. Damage inside the element has been simulated by attributing the local conductivity constants to the level of 0.1% of the corresponding "non-damaged" values. For illustration, the normalized conductivity along the local ply coordinates is set equal to unity along 1-direction and equal to 0.0013 in the 2- and 3-directions. Figure 1 shows the 3-D current flow distribution and 3-D voltage distribution as a sequence of contour plots in a set of cross sections of the laminated plate in the presence of delamination. The horizontal slices on the plots correspond to various interfaces between plies, as marked in the figure. Substantial difference around the damage as seen in the contour plots creates the basis for the damage detection system.
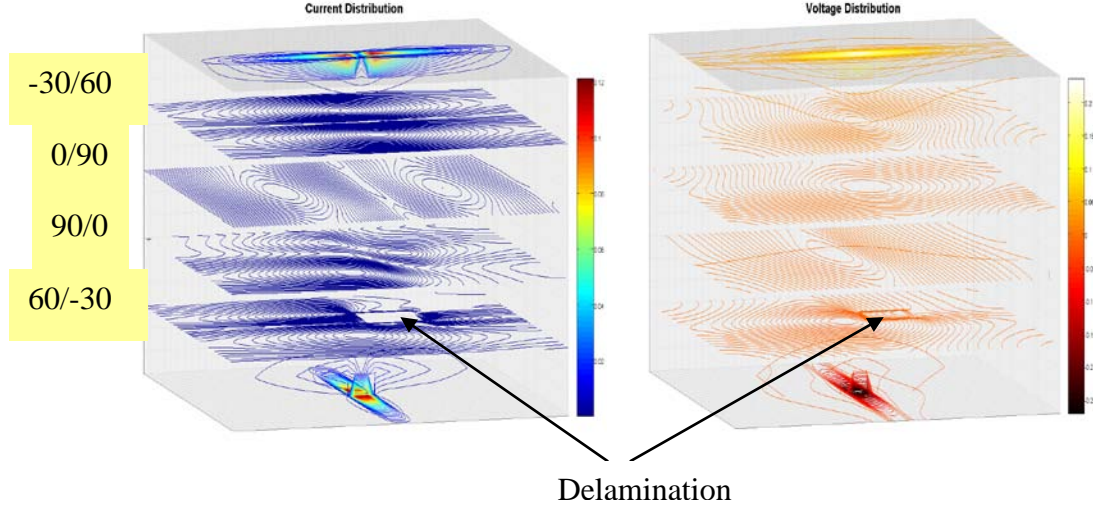

Figure 1: 3-D current distribution (left) and 3-D voltage distribution (right) in a delaminated rectangular plate

As a second example, we created a 2-D model of an isotropic plate with internal damage, as seen in Figure 2. For illustration, we assumed unit conductivity values in the undamaged region of the plate and assigned a value of 0.001 in the damaged zone. Figure 2 illustrates 2-D contour lines in the undamaged and damaged plates. Similar to the results of the 3-D example shown in Figure 1, we again observe substantial differences around the damage zone which forms the basis for the damage detection system.
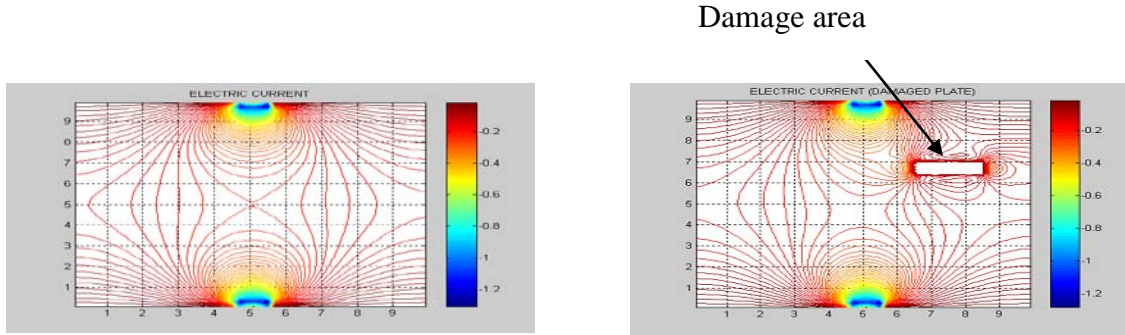
Damage area

Figure 2: 2-D current contour lines in the undamaged (left) and damaged (right) isotropic rectangular plate

2.0 Resistivity Measurement Test Bed

The technique requires a network of electrodes to apply electric potentials to the external surfaces of the structure (see Figure 3 as an example). By monitoring the integral resistance of the structure, observed changes in the baseline set of measurements can be related to the location and extent of any damage present.
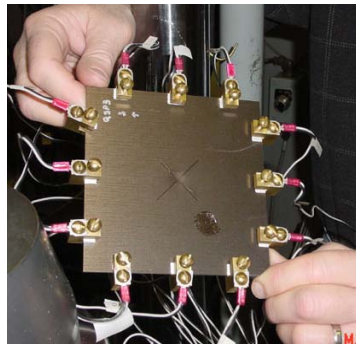

Figure 3: Network of Electrodes on a Composite plate

The data acquisition system for resistance measurement consists of two *Keithley* Model 7011-S Quad 1x10 Multiplexer boards housed in a *Keithley* Model 7001 Switching System mainframe, a *Keithley* Model 2400 Source Meter, and a *Keithley* Model 2182 7½-digit Digital Nanovoltmeter. Each multiplexer board contains 40 relays for channel switching. The wiring is arranged such that one multiplexer board is used for positive electrode selection and the second for negative ones. Each electrode has two wires connected to it: one for current source and one for voltage sense. The switching of these two wires is always in tandem. This arrangement allows for selection of any pair of positive/negative electrodes out of a total of 40 electrodes for 4-wire resistance measurements. The source meter provides the current source and the voltage is measured by the nanovoltmeter. To perform resistance measurements on a test panel, the data acquisition devices are placed under software control. A *MS Visual Basic* program has been developed for automating the electrode selection and resistance measurement process such that the resistance between any two electrodes can be measured as

commanded. It also provides the required capability for automatically scanning all combinations of any two electrodes.

Static indentation experiments were performed using 1" spherical indenter on quasi-isotropic panel. Figure 4 depicts the test set up for static indentation. The resistivity measurements can be made under loading so that changes in resistivity values could be related to the initiation and growth of damage.
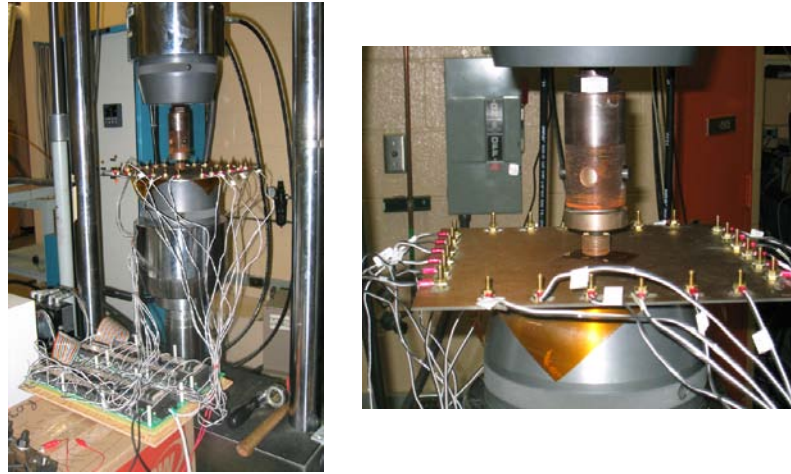

Figure 4: Test Set-up for Static Indentation

3.0 Model Validation

The numerical model was first verified against known analytical solutions, applying different symmetric and anti-symmetric Dirichlet/Neiman boundary conditions. It takes about 6 minutes to converge solution on a mesh 100 x 100 x 16 (relative residual drop is 0.000001) on a PC Pentium 4, CPU 1.4 GHz.

To validate the numerical results, experimental data was obtained from the static indentation experiment using three electrodes placed on each edge of [0/+-45/90]$_{2s}$ quasi-isotropic panel (Figure 3). The material system used is a carbon fiber-reinforced toughened bismaleimide, IM7/5250-4. A subset of 18 measurements was selected from the total 66 pairwise resistance measurements made. Physical constants, i.e., conductivity tensor for the unidirectional ply, were calibrated based on undamaged plate testing, i.e, from resistance measurements obtained prior to application of indentor load. It was determined from the 2-D numerical model that the in-plane conductivity values were 6.35 S/in and 6.95 S/in in the x and y directions, respectively. Under monotonic loading, electrical resistivity measurements were made by interrupting and holding the load at several pre-defined load steps. Loading was stopped when significant acoustic emission activity was observed in an attempt to obtain only sub-surface damage. Figure 5(a) is a C-scan of the composite plate at the end of loading. The observed damage in the composite plate was simulated as a through – hole damage in the shape of a square (side length 0.8"), as shown in Figure 5(b), with an assigned conductivity 0.1% of the undamaged value. Resistance signature (the difference between tested and simulated results) across the plate

in different directions for the undamaged and damaged plates is shown in Fig.6. Analytical solution for the undamaged plate matches testing data within the accuracy of 5%. For the damaged plate 16 out of 18 testing data reveal the same accuracy, within 5%, whereas prediction of the test data # 7 and #11 exceeds testing measurements by 9%. The latter could be attributed to the inhomogeneity within the computational domain, or to the highly variable contact resistances at the electrodes.
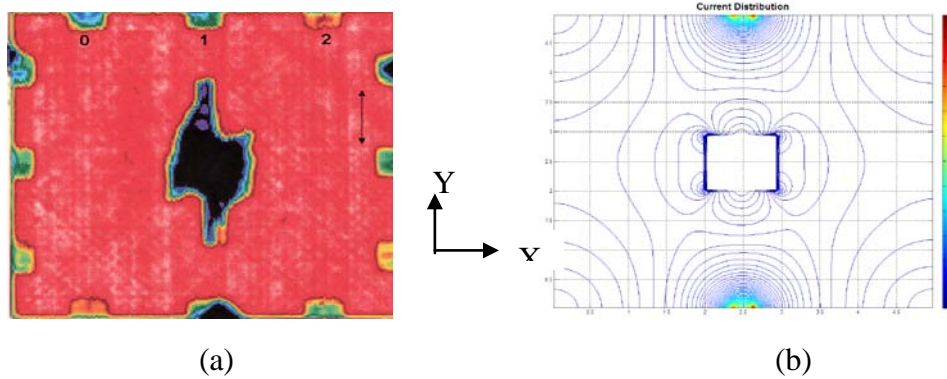

(a)   (b)

Figure 5: (a) C-scan image of observed damage, (b) simulated damage in 2-D model
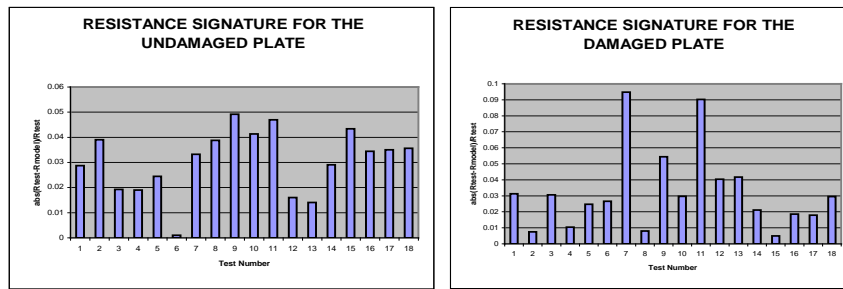

Figure 6: Testing Versus Prediction Data for the Undamaged (left) and
Damaged (right) Plates

Another example of code verification is presented in the form of delamination damage in IM7/5250-4 composites. Coupon specimens (12" long, 1" wide) of quasi-isotropic [0/45/90/-45]$_S$ laminate with various sizes of artificial delaminations obtained by inserting Teflon film at the laminate mid-plane were manufactured and the resistance were measured. A delamination area of 1.6" was introduced as shown in Figure 7, and the resistance for several different couples of active electrodes was calculated using theoretical model. The predicted and experimental resistance is shown in Figure 8 for various combinations of active electrodes. The corresponding contour lines for undamaged and damaged laminate are presented in Figure 9.
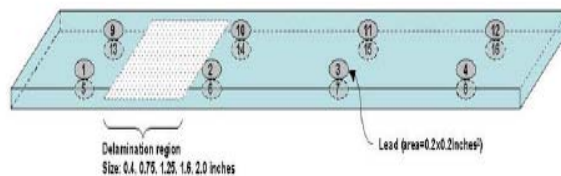

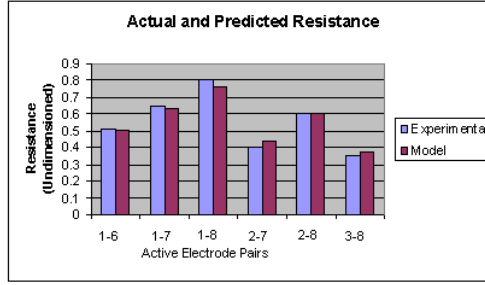Figure 7: Schematic of a quasi-isotropic laminate with embedded internal delamination

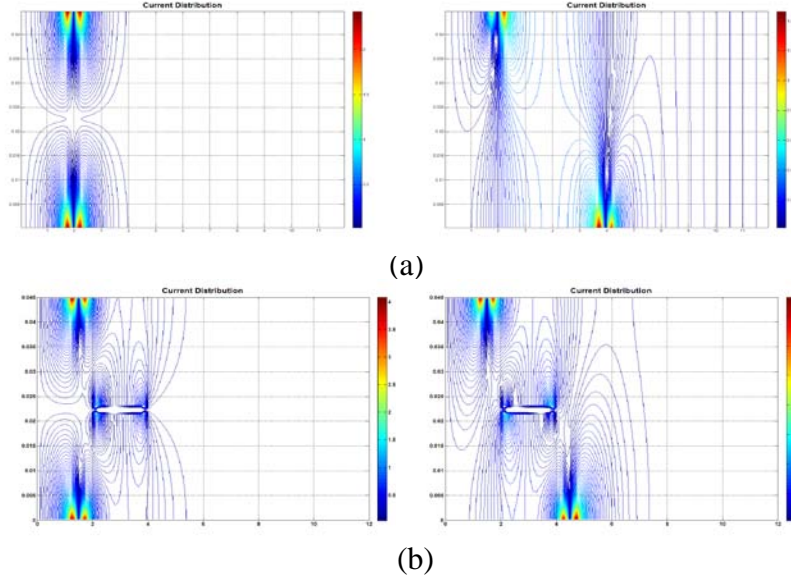Figure 8: Experimental and predicted resistance

(a)

(b)

Figure 9: Electrical current contour lines for 1-5 (left) and 1-6 (right) active lead pairs for (a) undamaged laminate and (b) laminate with embedded delamination

4.0   Damage Detection

The fundamental idea of damage detection is that through application of electrical voltage and recording electrical resistance, the mechanical condition of the electrically conductive structure can be detected. The damage is linked to the changes of local conductivity, which is appropriate for fiber breakage, tear or delamination of the composite laminate. Two schemes have been created for damage mapping. The first uses multiple simulation based look-up tables, attributing the coordinates and the size of the damage to the set of N*(N-1)/2 integral resistance measurements, where N is the number of the electrodes on each side of the plate. This approach is computationally expensive, but could be used to represent an arbitrary number of the damage sites.

Another approach is based on a neural network architecture. A feed-forward neural network is trained based on the location and the damage size. One thousand numerical simulations for the different damage sizes and locations were used in the training process. A flow chart of the neural network developed is presented in Figure 10 for a simulated damage scenario in a composite plate with a through–hole damage. Four neural networks were created simulating Cartesian coordinates for the center of through-hole damage, and

the size of the damage. Input data is a set of N*(N-1)/2 residuals, representing the differences of the resistances between active couples of the electrodes in the damaged and undamaged plates. Seventy-five percent of the cases are used in the training process while the rest are used for validation testing. In training the cell grid neural networks, 300 epochs of the training are executed before the validation set is introduced and the difference between network output and verified outcome becomes appropriate (Figure 10)
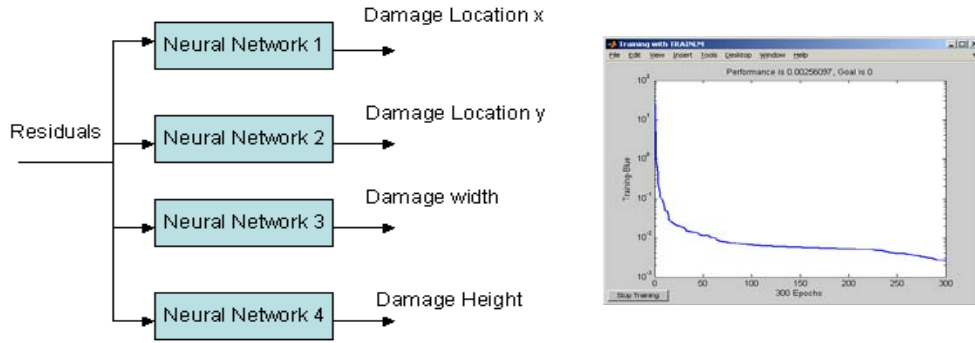

Figure 10: Training Neural Network

The result for damage detection is given in Figure 11 where the circle indicates the actual damage while the square is the prediction. The predicted (X, Y) coordinates of the hole are (1.8",6.8") versus actual coordinates (2.25",6.75"). In terms of the plate size (12" square), the accuracy in prediction of the through-hole center is 3.5% for a 3" through-hole diameter.
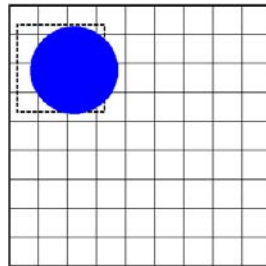

Figure 11: Comparison of Damage Prediction with Experimental Measurements

5.0   Conclusions

The achieved results indicate that the resistance based health monitoring system can be used to detect defects in electrically conductive composite systems. The coupled electromechanical models of damage hold considerable potential for guiding the development of these materials for both in-situ and ex-situ real-time damage sensors in a wide range of structural components where health monitoring is critical to both safety and cost-effective application of composites.